Training-free Diffusion Model Adaptation for Variable-Sized Text-to-Image Synthesis (Supplementary Materials)

Zhiyu Jin[1], **Xuli Shen**[1,2], **Bin Li**[1*], **Xiangyang Xue**[1]
[1] Shanghai Key Laboratory of Intelligent Information Processing
School of Computer Science, Fudan University
[2] UniDT Technology

In the Supplementary Materials, we first provide the proofs of the main conclusions in Section 3, then we introduce the involved existing assets, evaluation settings and computing infrastructure, and finally we show the additional experimental results on our method for the performance comparison.

Contents

1 Proofs

In this section, we provide the proofs of the connection between attention entropy and token number, which constitutes the main conclusion in Section 3.

Let $\mathbf{X} \in \mathbb{R}^{N \times d}$ denotes an image token sequence to an attention module, where N, d are the number of tokens and the token dimension, respectively. We then denote the key, query and value matrices as $\mathbf{K} = \mathbf{X}\mathbf{W}^K$, $\mathbf{Q}$ and $\mathbf{V}$, where $\mathbf{W}^K \in \mathbb{R}^{d \times d_r}$ is a learnable projection matrix. The attention layer ([2, 11]) computes Attention$(\mathbf{Q}, \mathbf{K}, \mathbf{V}) = \mathbf{A}\mathbf{V}$ with the attention map $\mathbf{A}$ calculated by the row-wise softmax function as follows:

$$\mathbf{A}_{i,j} = \frac{e^{\lambda \mathbf{Q}_i \mathbf{K}_j^\top}}{\sum_{j'=1}^{N} e^{\lambda \mathbf{Q}_i \mathbf{K}_{j'}^\top}}, \tag{1}$$

[*] Corresponding author

37th Conference on Neural Information Processing Systems (NeurIPS 2023).

where λ is a scaling factor, usually set as $1/\sqrt{d}$ in the widely-used Scaled Dot-Product Attention [11] and i, j are the row indices on the matrices $\mathbf{Q}$ and $\mathbf{K}$, respectively. Following [1, 4], we calculate the attention entropy by treating the attention distribution of each token as a probability mass function of a discrete random variable. The attention entropy with respect to i^{th} row of $\mathbf{A}$ is defined as:

$$\text{Ent}(\mathbf{A}_i) = -\sum_{j=1}^{N} \mathbf{A}_{i,j} \log(\mathbf{A}_{i,j}), \tag{2}$$

We now investigate the relation between the attention entropy and the token number. By substituting Eq.(1) into Eq.(2), we have:

$$\begin{aligned}
\text{Ent}(\mathbf{A}_i) &= -\sum_{j=1}^{N} \Big[\frac{e^{\lambda \mathbf{Q}_i \mathbf{K}_j^\top}}{\sum_{j`=1}^{N} e^{\lambda \mathbf{Q}_i \mathbf{K}_{j'}^\top}} \log\big(\frac{e^{\lambda \mathbf{Q}_i \mathbf{K}_j^\top}}{\sum_{j`=1}^{N} e^{\lambda \mathbf{Q}_i \mathbf{K}_{j'}^\top}}\big)\Big] \\
&= \log \sum_{j`=1}^{N} e^{\lambda \mathbf{Q}_i \mathbf{K}_{j'}^\top} - \frac{\sum_{j=1}^{N} \big(e^{\lambda \mathbf{Q}_i \mathbf{K}_j^\top} \lambda \mathbf{Q}_i \mathbf{K}_j^\top\big)}{\sum_{j`} e^{\lambda \mathbf{Q}_i \mathbf{K}_{j'}^\top}} \\
&= \log N + \log\big(\frac{1}{N} \sum_{j=1}^{N} e^{\lambda \mathbf{Q}_i \mathbf{K}_j^\top}\big) - \frac{\frac{1}{N} \sum_{j=1}^{N} \big(e^{\lambda \mathbf{Q}_i \mathbf{K}_j^\top} \lambda \mathbf{Q}_i \mathbf{K}_j^\top\big)}{\frac{1}{N} \sum_{j} e^{\lambda \mathbf{Q}_i \mathbf{K}_j^\top}} \\
&\approx \log N + \log \mathbb{E}_j\big(e^{\lambda \mathbf{Q}_i \mathbf{K}_j^\top}\big) - \frac{\mathbb{E}_j\big(\lambda \mathbf{Q}_i \mathbf{K}_j^\top e^{\lambda \mathbf{Q}_i \mathbf{K}_j^\top}\big)}{\mathbb{E}_j\big(e^{\lambda \mathbf{Q}_i \mathbf{K}_j^\top}\big)},
\end{aligned} \tag{3}$$

where $\mathbb{E}_j$ denotes the expectation upon the index j, and the last equality holds asymptotically when N gets larger.

Given $\mathbf{X}$ as an encoded sequence from an image, we assume each token $\mathbf{X}_j$ as a vector sampled from a multivariate Gaussian distribution $\mathcal{N}(\boldsymbol{\mu}^X, \boldsymbol{\Sigma}^X)$. This widespread assumption is shared by multiple works [5, 6, 7] in image synthesis and style transfer. In this way, each $\mathbf{K}_j = \mathbf{X}_j \mathbf{W}^K$ could be considered as a sample from a multivariate Gaussian distribution $\mathcal{N}(\boldsymbol{\mu}^K, \boldsymbol{\Sigma}^K) = \mathcal{N}(\boldsymbol{\mu}^X \mathbf{W}^K, (\mathbf{W}^K)^\top \boldsymbol{\Sigma}^X \mathbf{W}^K)$. In regard to $\mathbf{K}_j$, its dimension-wise linear combination $y_i = \lambda \mathbf{Q}_i \mathbf{K}_j^\top$ could be treated as a scalar random variable sampled from a Gaussian distribution $y_i \sim \mathcal{N}(\mu_i, \sigma_i^2) = \mathcal{N}(\lambda \mathbf{Q}_i (\boldsymbol{\mu}^K)^\top, \lambda^2 \mathbf{Q}_i \boldsymbol{\Sigma}^K \mathbf{Q}_i^\top)$. Under this circumstance, we dive into the expectations $\mathbb{E}_j\big(e^{\lambda \mathbf{Q}_i \mathbf{K}_j^\top}\big)$ and $\mathbb{E}_j\big(\lambda \mathbf{Q}_i \mathbf{K}_j^\top e^{\lambda \mathbf{Q}_i \mathbf{K}_j^\top}\big)$ in Eq.(3):

$$\begin{aligned}
\mathbb{E}_j\big(e^{\lambda \mathbf{Q}_i \mathbf{K}_j^\top}\big) &\doteq \mathbb{E}_j\big(e^{y_i}\big) \\
&= \int e^{y_i} \frac{1}{\sqrt{2\pi}\sigma_i} e^{-\frac{y_i^2 - 2\mu_i y_i + \mu_i^2}{2\sigma_i^2}} dy_i \\
&= \int \frac{1}{\sqrt{2\pi}\sigma_i} e^{-\frac{(y_i - \mu_i - \sigma_i^2)^2}{2\sigma_i^2}} e^{\mu_i + \frac{\sigma_i^2}{2}} dy_i \\
&= e^{\mu_i + \frac{\sigma_i^2}{2}} \\
\mathbb{E}_j\big(\lambda \mathbf{Q}_i \mathbf{K}_j^\top e^{\lambda \mathbf{Q}_i \mathbf{K}_j^\top}\big) &\doteq \mathbb{E}_j\big(y_i e^{y_i}\big) \\
&= \int y_i e^{y_i} \frac{1}{\sqrt{2\pi}\sigma_i} e^{-\frac{y_i^2 - 2\mu_i y_i + \mu^2}{2\sigma^2}} dy_i \\
&= \int y_i \frac{1}{\sqrt{2\pi}\sigma_i} e^{-\frac{(y_i - \mu_i - \sigma_i^2)^2}{2\sigma_i^2}} e^{\mu_i + \frac{\sigma_i^2}{2}} dy_i \\
&= \big(\mu_i + \sigma_i^2\big) e^{\mu_i + \frac{\sigma_i^2}{2}},
\end{aligned} \tag{4}$$

By substituting Eq.(4) into Eq.(3), we have:

$$\begin{aligned}\mathrm{Ent}(\mathbf{A}_i) &= \log N + \log\left(e^{\mu_i+\frac{\sigma_i^2}{2}}\right) - \frac{\left(\mu_i+\sigma_i^2\right)e^{\mu_i+\frac{\sigma_i^2}{2}}}{e^{\mu_i+\frac{\sigma_i^2}{2}}} \\ &= \log N + \mu_i + \frac{\sigma_i^2}{2} - \left(\mu_i+\sigma_i^2\right) \\ &= \log N - \frac{\sigma_i^2}{2}.\end{aligned} \tag{5}$$

In this way, we reach the connection between attention entropy and token number, which lays a solid theoretical foundation for the subsequent interpretations and the scaling factor proposed.

2 Implementation details

In this section, we provide the detailed implementation settings in Section 4, including involved existing assets, evaluation settings, computing infrastructure, etc.

2.1 Involved existing assets.

For the evaluation code, we refer to the github code repository called Diffusers (URL) released by Hugging face with Apache License, Version 2.0. The revised code are shown in Algorithm 1.

For the model parameters, we select the stable diffusion parameters released by stability AI ([8], version: stable-diffusion-2-1-base, URL) and the latent diffusion parameters released by CompVis ([8], version: ldm-text2im-large-256, URL). Both of them are top-ranked parameter files for downloading.

For datasets, we use `LAION-400M` ([10], URL) and `LAION-5B` dataset ([9], URL), which contain over 400 million and 5.85 billion CLIP-filtered image-text pairs, respectively.

Algorithm 1 Replace the scaling factor

```
Require: Token number during training $\mathbf{T} \geq 0$, Flag to replace the scaling factor $C$
Ensure: $\lambda = \sqrt{\log_T N/d}$
  $\mathbf{Q} \leftarrow \mathbf{X}\mathbf{W}_Q$
  $\mathbf{K} \leftarrow \mathbf{X}\mathbf{W}_K$
  $\mathbf{V} \leftarrow \mathbf{X}\mathbf{V}_V$
  if $C$ is True then
      $\lambda \leftarrow \sqrt{\log_T N/d}$
  else if $C$ is False then
      $\lambda \leftarrow \sqrt{1/d}$
  end if
  Attn = softmax($\lambda\mathbf{Q}\mathbf{K}^\top$)$\mathbf{V}$
```

2.2 Evaluation settings

We evaluate two scaling factors on a subset of `LAION-400M` and `LAION-5B` dataset. We randomly select 30K image-text data pairs from `LAION-5B` and 50K image-text data pairs from `LAION-400M`, respectively. We then synthesize corresponding 30K images upon `LAION-5B` text data with stable diffusion model and 50K images upon `LAION-400M` text data with latent diffusion model. We compute corresponding FID-30K (Stable diffusion) and FID-50k (Latent diffusion) with synthesized images and original images from datasets.

2.3 Computing infrastructure

Experiments are conducted on a server with Intel(R) Xeon(R) Gold 6226R CPUs @ 2.90GHz and four NVIDIA Tesla A100 GPUs. The code is developed based on the PyTorch framework with version 1.9.1.

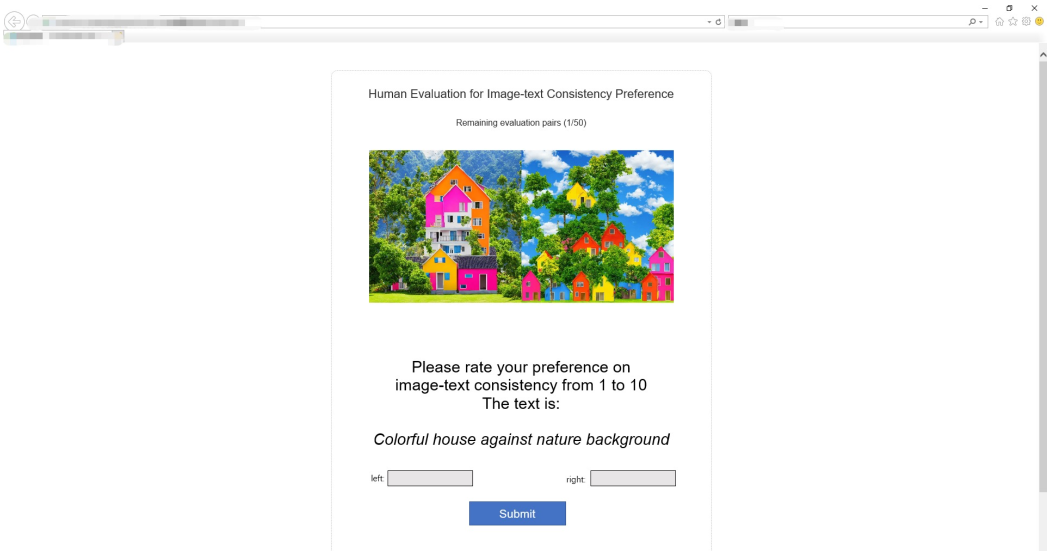

Human Evaluation for Image-text Consistency Preference

Remaining evaluation pairs (1/50)

Please rate your preference on
image-text consistency from 1 to 10
The text is:

Colorful house against nature background

Figure 1: The screenshot of our human evaluation website.

2.4 Human evaluation details

We conduct an text-based pairwise preference test. For a specific context, we pair the synthesized image of our method with the synthesized image from the baseline and ask 45 annotators to give each response a rating score for consistency. We randomly select 50 pairs of images-text data (two images from two methods and a corresponding text prompt) and show them to 45 participants to rate from 1 to 10. We observe that users rate higher for our method, which suggests that the synthesized images from our method are more contextually coherent with texts than the baseline. Besides, with the refinement from the proposed scaling factor, the generated contents from our model are able to convey more natural and informative objects. The screenshot is depicted in Figure 1.

3 Broader impacts

Our approach focuses on synthesizing images with a high level of fidelity, which raises concerns about potential impacts in a broader context, specifically related to the misuse of portraits. Notably, when our method is provided with prompts referencing highly popular celebrities, it consistently generates figures that bear a strong resemblance to the mentioned individuals. Consequently, there is a risk of portrait misusing or even the infringement of portrait rights.

It is worth acknowledging that the potential impact mentioned above is not unique to our method but is a challenge faced by most image synthesis techniques. We firmly believe that numerous researchers have already recognized and been working on this issue with utmost seriousness and diligence.

4 Additional experimental results

In this section, we provide more qualitative and quantitative results for the validation of our theoretical findings and the proposed scaling factor.

4.1 Qualitative results

As shown in Figure 2, 3 and 4, our scaling factor manages to synthesize objects with better visual effect in lower resolution images, outperforming the original scaling which depicts visual concepts in a rough manner. From Figure 5 and 6, our scaling factor does better in naturally organizing visual concepts portrayal in higher resolution images, surpassing the original scaling factor in image presentations.

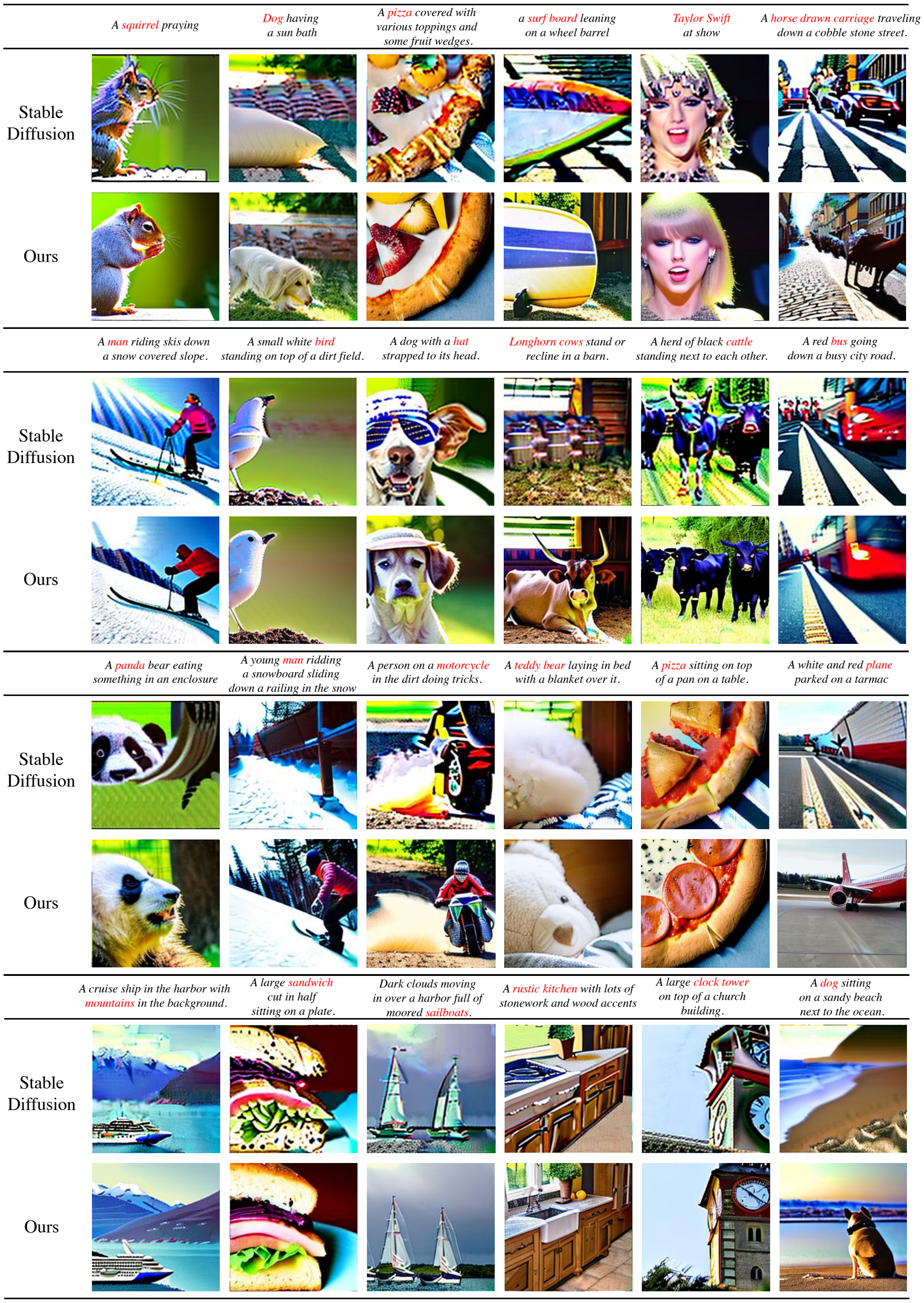
A squirrel praying
Dog having a sun bath
A pizza covered with various toppings and some fruit wedges.
a surf board leaning on a wheel barrel
Taylor Swift at show
A horse drawn carriage traveling down a cobble stone street.
Stable Diffusion
Ours
A man riding skis down a snow covered slope.
A small white bird standing on top of a dirt field.
A dog with a hat strapped to its head.
Longhorn cows stand or recline in a barn.
A herd of black cattle standing next to each other.
A red bus going down a busy city road.
Stable Diffusion
Ours
A panda bear eating something in an enclosure
A young man ridding a snowboard sliding down a railing in the snow
A person on a motorcycle in the dirt doing tricks.
A teddy bear laying in bed with a blanket over it.
A pizza sitting on top of a pan on a table.
A white and red plane parked on a tarmac
Stable Diffusion
Ours
A cruise ship in the harbor with mountains in the background.
A large sandwich cut in half sitting on a plate.
Dark clouds moving in over a harbor full of moored sailboats.
A rustic kitchen with lots of stonework and wood accents
A large clock tower on top of a church building.
A dog sitting on a sandy beach next to the ocean.
Stable Diffusion
Ours

Figure 2: **Qualitative comparison** on the scale factors for the resolution 224 × 224. The original scaling factor misses out content or roughly depicts the objects in prompts while our scaling factor manages to synthesize visual concepts in high fidelity and better illumination. Please zoom in for better visual effect.

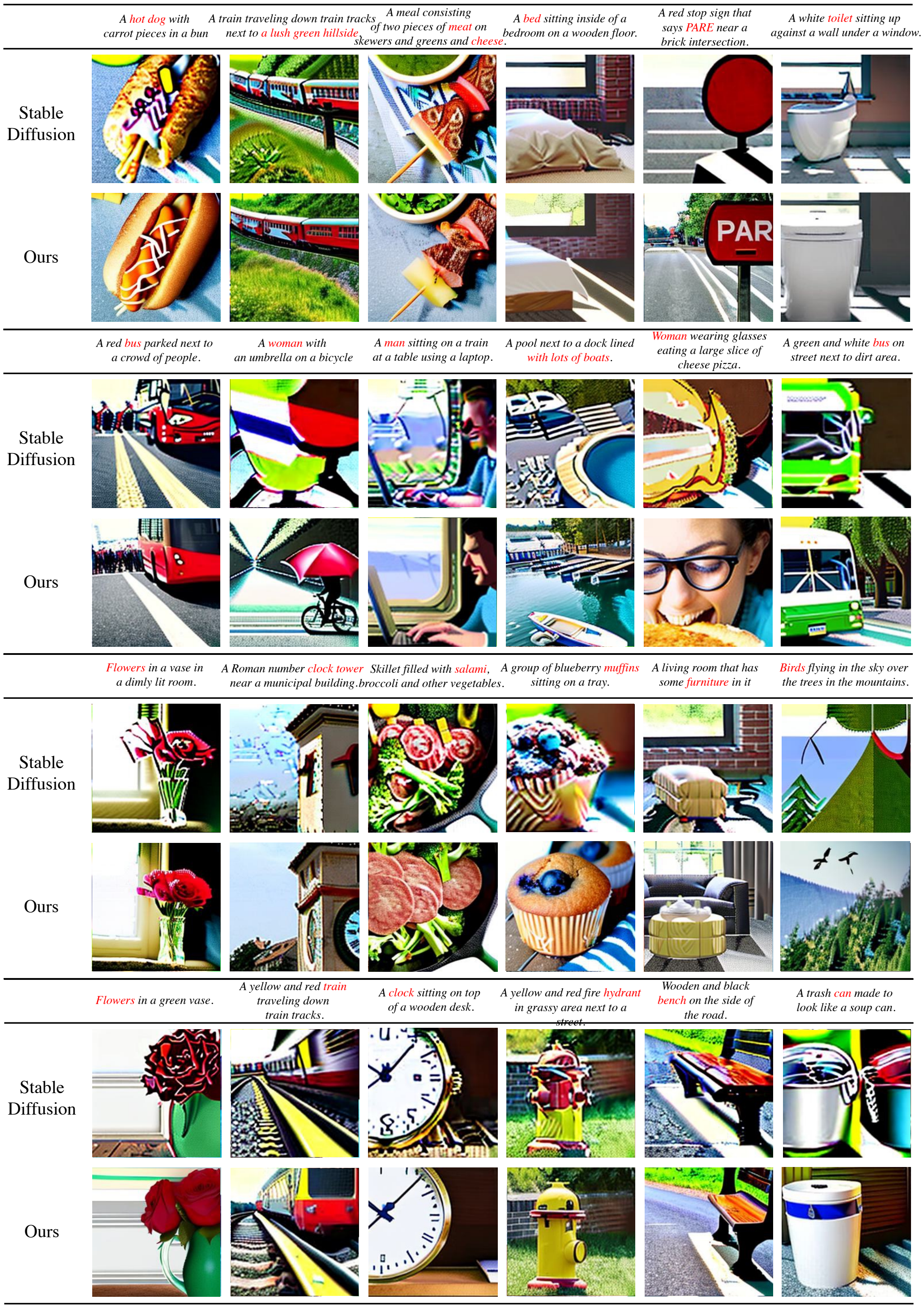
A hot dog with carrot pieces in a bun
A train traveling down train tracks next to a lush green hillside.
A meal consisting of two pieces of meat on skewers and greens and cheese.
A bed sitting inside of a bedroom on a wooden floor.
A red stop sign that says PARE near a brick intersection.
A white toilet sitting up against a wall under a window.
Stable Diffusion
Ours
PAR
A red bus parked next to a crowd of people.
A woman with an umbrella on a bicycle
A man sitting on a train at a table using a laptop.
A pool next to a dock lined with lots of boats.
Woman wearing glasses eating a large slice of cheese pizza.
A green and white bus on street next to dirt area.
Stable Diffusion
Ours
Flowers in a vase in a dimly lit room.
A Roman number clock tower near a municipal building.
Skillet filled with salami, broccoli and other vegetables.
A group of blueberry muffins sitting on a tray.
A living room that has some furniture in it
Birds flying in the sky over the trees in the mountains.
Stable Diffusion
Ours
Flowers in a green vase.
A yellow and red train traveling down train tracks.
A clock sitting on top of a wooden desk.
A yellow and red fire hydrant in grassy area next to a street.
Wooden and black bench on the side of the road.
A trash can made to look like a soup can.
Stable Diffusion
Ours

Figure 3: **Qualitative comparison** on the scale factors for the resolution 224 × 224. The original scaling factor misses out content or roughly depicts the objects in prompts while our scaling factor manages to synthesize visual concepts in high fidelity and better illumination. Please zoom in for better visual effect.

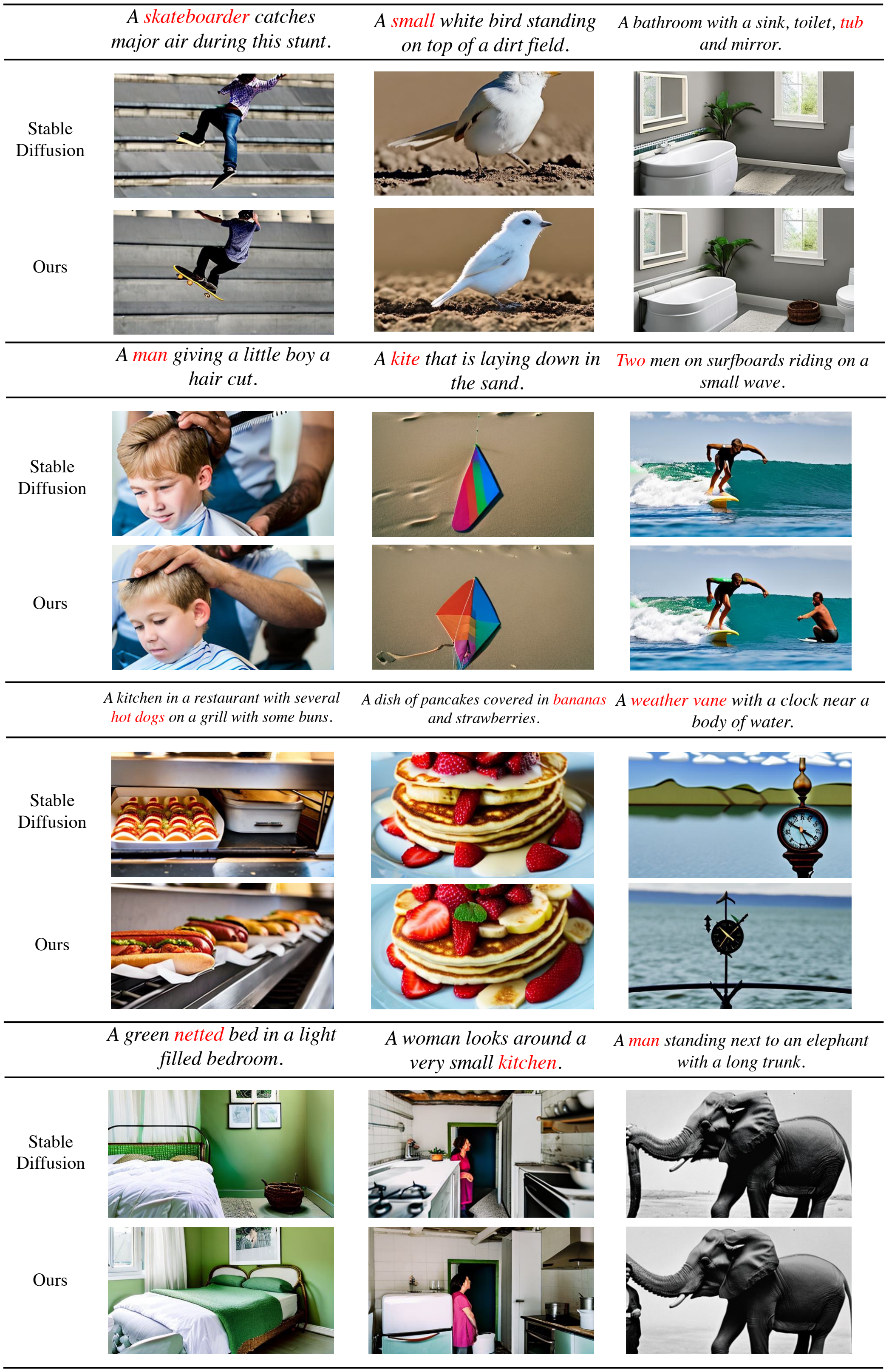
A skateboarder catches major air during this stunt.
A small white bird standing on top of a dirt field.
A bathroom with a sink, toilet, tub and mirror.
Stable Diffusion
Ours
A man giving a little boy a hair cut.
A kite that is laying down in the sand.
Two men on surfboards riding on a small wave.
Stable Diffusion
Ours
A kitchen in a restaurant with several hot dogs on a grill with some buns.
A dish of pancakes covered in bananas and strawberries.
A weather vane with a clock near a body of water.
Stable Diffusion
Ours
A green netted bed in a light filled bedroom.
A woman looks around a very small kitchen.
A man standing next to an elephant with a long trunk.
Stable Diffusion
Ours

Figure 4: **Qualitative comparison** on the scale factors for the resolution 512 × 288. The original scaling factor misses out content or roughly depicts the objects in prompts while our scaling factor manages to synthesize visual concepts in high fidelity and better illumination. Please zoom in for better visual effect.

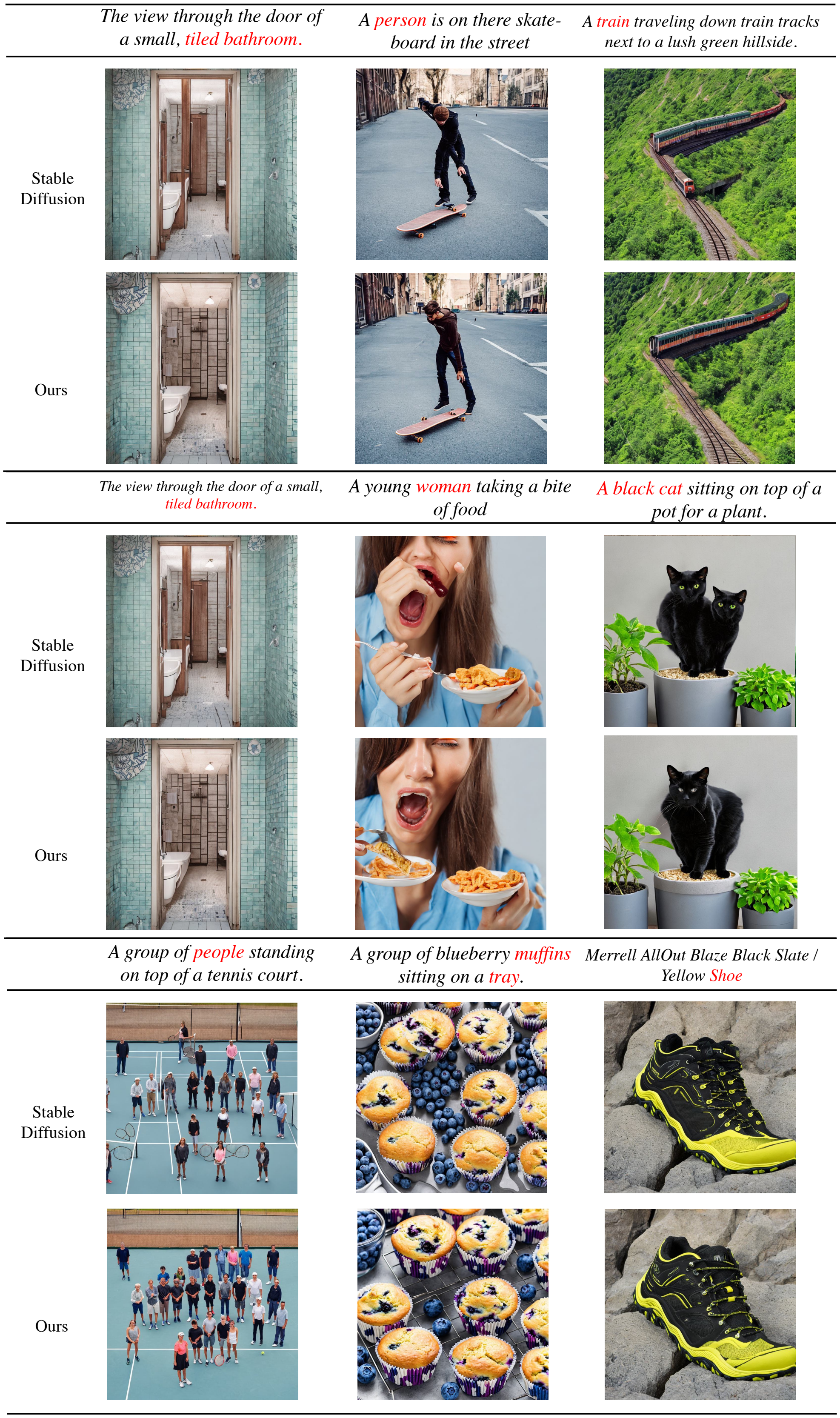
The view through the door of a small, tiled bathroom.
A person is on there skate-board in the street
A train traveling down train tracks next to a lush green hillside.
Stable Diffusion
Ours
The view through the door of a small, tiled bathroom.
A young woman taking a bite of food
A black cat sitting on top of a pot for a plant.
Stable Diffusion
Ours
A group of people standing on top of a tennis court.
A group of blueberry muffins sitting on a tray.
Merrell AllOut Blaze Black Slate / Yellow Shoe
Stable Diffusion
Ours

Figure 5: **Qualitative comparison** on the scale factors for the resolution 768 × 768. The original scaling factor depicts the objects in a repetitive and unorganized pattern while our scaling factor manages to synthesize visual concepts in high fidelity. Please zoom in for better visual effect.

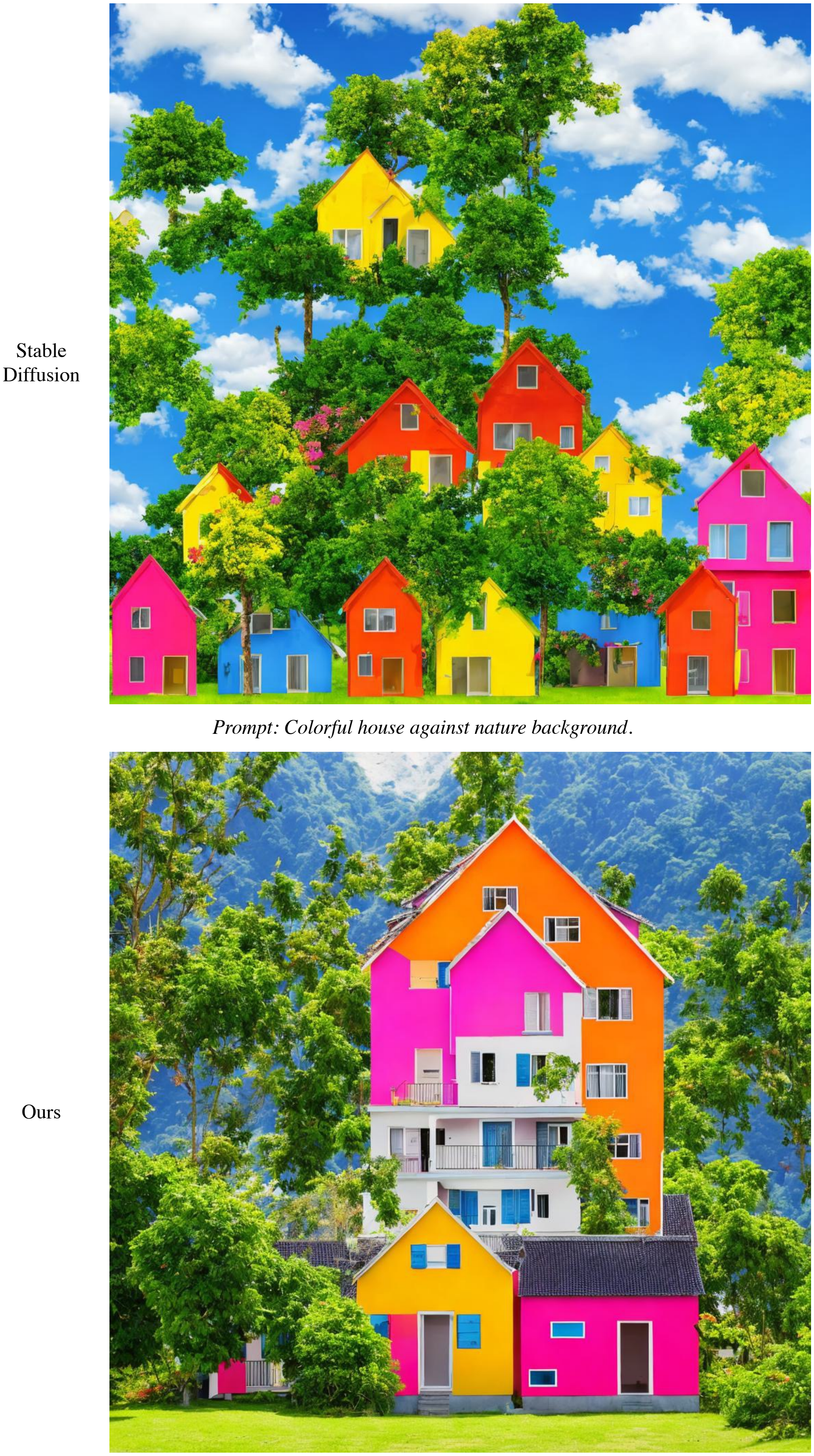

Prompt: Colorful house against nature background.

Figure 6: **Qualitative comparison** on the scale factors for the resolution 1024×1024.

Table 1: FID, memory usage and time cost of stable diffusion with multiple settings for different resolutions. The results for low resolution demonstrate that our method could achieve better performance in memory usage and time cost with trade-off in fidelity.

Resoluions	**FID** (↓)	**GPU Memory (MiB)** (↓)	**Average Time (s)** (↓)
128 * 128 (Original)	191.5447	**6867**	**3.4953**
128 * 128 (Ours)	127.2798	**6867**	3.4955
512 * 512 and Resize to 128	**36.0742**	9324	17.4377
224 * 224 (Original)	74.5742	**7064**	**5.6268**
224 * 224 (Ours)	41.8925	**7064**	5.6274
512 * 512 and Resize to 224	**21.8415**	9324	17.4457

Table 2: FID (4K samples), memory usage and time cost of our method and MultiDiffusion[3]. Our method outperforms MultiDiffusion on each metric except for the GPU Memory.

Resoluions	**FID** (↓)	**GPU Memory (MiB)** (↓)	**Average Time (s)** (↓)
224 * 224 (Ours)	**50.3515**	7064	**5.6274**
224 * 224 (MD)	154.6925	**7061**	31.7680
768 * 768 (Ours)	**28.1372**	19797	**36.7140**
768 * 768 (MD)	40.9270	**9906**	122.2485

4.2 Quantitative results

In Table 1, we present FID, memory usage and time cost of stable diffusion with multiple settings for the text-to-image synthesis of various resolutions $(128^2, 224^2, 768^2, 1024^2)$. For low resolution, our method achieves better performance in memory usage and time cost with trade-off in fidelity. Considering the high demand for memory and time resources (especially for portable devices), we believe the trade-off is acceptable.

In Table 2, We compare our method with MultiDiffusion[3] and report corresponding FID(4K samples), memory usage and time cost. As it is shown, our method outperforms MultiDiffusion on each metric except for the GPU Memory.

References

[1] Giuseppe Attanasio, Debora Nozza, Dirk Hovy, and Elena Baralis. Entropy-based attention regularization frees unintended bias mitigation from lists. *arXiv preprint arXiv:2203.09192*, 2022.

[2] Dzmitry Bahdanau, Kyunghyun Cho, and Yoshua Bengio. Neural machine translation by jointly learning to align and translate. *arXiv preprint arXiv:1409.0473*, 2014.

[3] Omer Bar-Tal, Lior Yariv, Yaron Lipman, and Tali Dekel. Multidiffusion: Fusing diffusion paths for controlled image generation. 2023.

[4] Hamidreza Ghader and Christof Monz. What does attention in neural machine translation pay attention to? *arXiv preprint arXiv:1710.03348*, 2017.

[5] Martin Heusel, Hubert Ramsauer, Thomas Unterthiner, Bernhard Nessler, and Sepp Hochreiter. Gans trained by a two time-scale update rule converge to a local nash equilibrium. *Advances in neural information processing systems*, 30, 2017.

[6] Xun Huang and Serge Belongie. Arbitrary style transfer in real-time with adaptive instance normalization. In *Proceedings of the IEEE international conference on computer vision*, pages 1501–1510, 2017.

[7] Ming Lu, Hao Zhao, Anbang Yao, Yurong Chen, Feng Xu, and Li Zhang. A closed-form solution to universal style transfer. In *Proceedings of the IEEE/CVF International Conference on Computer Vision*, pages 5952–5961, 2019.

[8] Robin Rombach, Andreas Blattmann, Dominik Lorenz, Patrick Esser, and Björn Ommer. High-resolution image synthesis with latent diffusion models. In *Proceedings of the IEEE/CVF Conference on Computer Vision and Pattern Recognition*, pages 10684–10695, 2022.

[9] Christoph Schuhmann, Romain Beaumont, Richard Vencu, Cade Gordon, Ross Wightman, Mehdi Cherti, Theo Coombes, Aarush Katta, Clayton Mullis, Mitchell Wortsman, et al. Laion-5b: An open large-scale dataset for training next generation image-text models. *arXiv preprint arXiv:2210.08402*, 2022.

[10] Christoph Schuhmann, Richard Vencu, Romain Beaumont, Robert Kaczmarczyk, Clayton Mullis, Aarush Katta, Theo Coombes, Jenia Jitsev, and Aran Komatsuzaki. Laion-400m: Open dataset of clip-filtered 400 million image-text pairs. *arXiv preprint arXiv:2111.02114*, 2021.

[11] Ashish Vaswani, Noam Shazeer, Niki Parmar, Jakob Uszkoreit, Llion Jones, Aidan N Gomez, Łukasz Kaiser, and Illia Polosukhin. Attention is all you need. *Advances in neural information processing systems*, 30, 2017.